Opto-Electronic Advances

Review

2022, Vol. 5, No. 5

DOI: 10.29026/oea.2022.210094

Single-molecule optoelectronic devices: physical mechanism and beyond

Peihui Li[1], Yijian Chen[1], Boyu Wang[1], Mengmeng Li[1], Dong Xiang[1]*, Chuancheng Jia[1]* and Xuefeng Guo[1,2]*

Single-molecule devices not only promise to provide an alternative strategy to break through the miniaturization and functionalization bottlenecks faced by traditional semiconductor devices, but also provide a reliable platform for exploration of the intrinsic properties of matters at the single-molecule level. Because the regulation of the electrical properties of single-molecule devices will be a key factor in enabling further advances in the development of molecular electronics, it is necessary to clarify the interactions between the charge transport occurring in the device and the external fields, particularly the optical field. This review mainly introduces the optoelectronic effects that are involved in single-molecule devices, including photoisomerization switching, photoconductance, plasmon-induced excitation, photovoltaic effect, and electroluminescence. We also summarize the optoelectronic mechanisms of single-molecule devices, with particular emphasis on the photoisomerization, photoexcitation, and photo-assisted tunneling processes. Finally, we focus the discussion on the opportunities and challenges arising in the single-molecule optoelectronics field and propose further possible breakthroughs.

Keywords: optoelectronic device; single-molecule junction; light-matter interaction; switch; electroluminescence; plasmon

Li PH, Chen YJ, Wang BY, Li MM, Xiang D et al. Single-molecule optoelectronic devices: physical mechanism and beyond. *Opto-Electron Adv* **5**, 210094 (2022).

Introduction

Single-molecule electronic devices, which use single molecules or molecular monolayers as their conductive channels, offer a new strategy to resolve the miniaturization and functionalization bottlenecks encountered by traditional semiconductor electronic devices[1–6]. These devices have many inherent advantages, including adjustable electronic characteristics, ease of availability, functional diversity and so on. To date, single-molecule devices with a variety of functions have been realized, including switches[7,8], field-effect devices[9,10], and optoelectronic devices[11,12]. In addition to their important applications in the functional device field, single-molecule devices also provide a unique platform to enable exploration of the chemical and physical laws of molecules at the single-molecule level.

Regulation of the electrical properties of single-molecule devices remains the key step toward further advancement in the development of molecular electronics. To adjust the molecular properties of the device

[1]Center of Single-Molecule Sciences, Institute of Modern Optics, Tianjin Key Laboratory of Micro-scale Optical Information Science and Technology, Frontiers Science Center for New Organic Matter, College of Electronic Information and Optical Engineering, Nankai University, Tianjin 300350, China; [2]Beijing National Laboratory for Molecular Sciences, State Key Laboratory for Structural Chemistry of Unstable and Stable Species, College of Chemistry and Molecular Engineering, Peking University, Beijing 100871, China.

*Correspondence: D Xiang, E-mail: xiangdongde@nankai.edu.cn; CC Jia, E-mail: jiacc@nankai.edu.cn; XF Guo, E-mail: guoxf@pku.edu.cn

Received: 24 July 2021; Accepted: 3 November 2021; Published online: 20 May 2022

efficiently, it is necessary to clarify the interactions between the electron transport in single-molecule devices and external fields, such as the external temperature[13,14], and the magnetic[15], electric[16–18], and light fields[7,19] etc. Among these fields, regulation of the electronic properties of single-molecule devices using light represents one of the most important fields, which is known as "single-molecule optoelectronics". This interaction not only refers to the effects of light on the electrical properties of molecular devices, i.e., control of the electron transport through the molecules using light, but also refers to the luminescence generated by the molecules during charge transfer. Understanding the photoelectric interaction mechanism in single-molecule devices will be of major significance for the development of single-molecule optoelectronics.

In this paper, we introduce the optoelectronic effects involved in single-molecule optoelectronic devices, including photoisomerization switching, photoconductance, plasmon-induced excitation, photovoltaic effect, and electroluminescence. The mechanisms of light in single-molecule functional devices are summarized, with particular emphasis on the photoisomerization, photoexcitation and photo-assisted tunneling processes. Finally, we analyze the potential challenges in the development of single-molecule optoelectronics and propose further research directions that may achieve the required breakthroughs in this field.

Single-molecule optoelectronic switches

Molecular switches have attracted considerable attention in the molecular electronics field because of their unlimited potential applications in areas including information storage, logical data manipulation and signal processing[20–22]. A typical molecular switch consists of a bistable molecular functional core and the anchoring groups required for covalent insertion of the functional molecule into metal or carbon electrodes[23]. Therefore, the design and synthesis processes of these switchable functional molecules have major research significance. Depending on the switching mechanism of the specific functional molecule, molecular switches can be divided into two types: conformation switches and charging/redox switches. In conformation switches, molecular conformational isomerization occurs as a result of changes in the chemical bonds. This conformational isomerization can be triggered reversibly using light, mechanical force, electric fields, temperature changes, and chemical reactants. One of the most commonly used triggering methods is light excitation, which provides a sensitive, convenient, and noninvasive way to control these switches. Photochromic molecules such as diarylethene, azobenzene, and spiropyran derivatives have been studied widely in single-molecule devices. These photochromic molecules have been shown to be promising as potential building blocks for molecular electronics. In general, single-molecule switches based on the break junction technologies have relatively poor stability, while switches based on single molecules connected to carbon-based electrodes through amide bonds can be stable for more than one year in the atmosphere. On the one hand, the Au-S bond is weaker than the amide bond. On the other hand, most switches based on break junctions are formed during the stretching process. In addition, for switches based on self-assembled monolayers (SAMs), the stability is promising due to the effective protection of SAMs between the electrodes. Here, we highlight the important progress made based on use of these molecules as classical light-driven molecular switches and provide basic discussions of their photophysical mechanisms.

Single-molecule diarylethene switches

In general, diarylethene derivatives undergo a 6π electron cyclization in the triene system under ultraviolet (UV) light stimulation and decyclization under visible (Vis) light irradiation, as shown in Fig. 1(a). Figure 1(b) shows the paths for ring opening and closing of the diarylethene molecule. The general structure for single-molecule devices is shown in Fig. 1(c), where the structure consists of metal or carbon electrodes and single diarylethene derivatives acting as the molecular conductive channels. These diarylethene derivatives exhibit photoelectric switching behaviors from an insulating state (the off state) to a highly conjugated state (the on state), which occurs because the cyclization generates a conjugated pathway for charge transfer through the molecules. Diarylethene derivatives are particularly attractive for applications in single-molecule junctions and molecular tunneling devices with SAMs because of their thermal stability, their high fatigue resistance and the sub-angstrom length differences between isomers.

Switching properties of single diarylethenes

Use of the technique of scanning tunneling microscope break junctions (STM-BJs) makes it possible to detect the specific conductance of individual photo-switchable

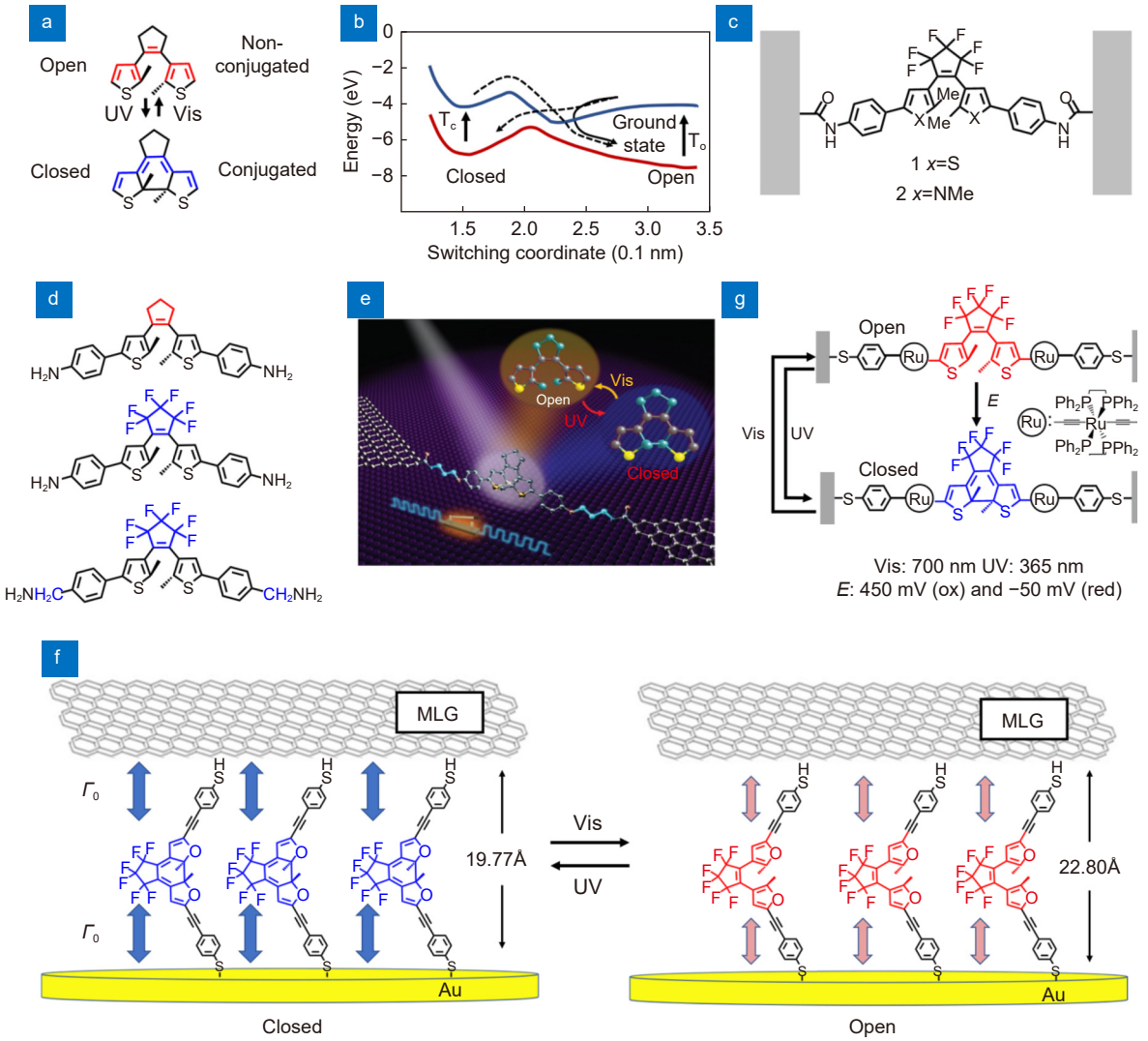

Fig. 1 | Diarylethene units used in single-molecule switches. (**a**) Diarylethene photoisomerization mechanism. (**b**) Potential energy curves of the molecular switching. The switching process is initiated by an excitation to the first excited state. (**c**) Diarylethene bridged between the electrode ends. (**d**) Molecular structures with special design for single-molecule switches. (**e**) A graphene-diarylethene-graphene single-molecule switch. (**f**) Self-assembled monolayer devices with diarylethene units. (**g**) Molecular isomerization under external controls of electrochemical potential and light irradiation. Figure reproduced with permission from: (a) ref.[24], American Chemical Society; (b) ref.[26], American Physical Society; (c) ref.[27], American Chemical Society; (d) ref.[28], John Wiley and Sones; (e) ref.[7], American Association for the Advancement of Science; (f) ref.[30], American Chemical Society; (g) ref.[32], under a Creative Commons Attribution 3.0 Unported Licence.

diarylethene molecules in both their conductive closed configuration and their non-conductive open configuration. In general, the closed configuration of diarylethene molecules has a higher conductance than the open configuration[24]. It should be noted here that individual molecules connected to the STM tip and to the gold substrate through pyridine groups have a fixed configuration and cannot undergo *in situ* configuration conversion. In addition, the effects of anchoring groups and bridging chains on the interface coupling strength and the conductance switching characteristics have been investigated using a mechanically controlled break junction (MCBJ) technology[25]. Specifically, the charge transport characteristics of molecules with various anchoring groups and bridging chains have been studied. In all cases, the single-molecule conductivity of the closed form molecule is higher than that of the open form. However, their conductance switching ratios (i.e., the ratio of the conductance of the closed form to that of the open form of the single molecule) are different. When the molecular π functional core is conjugated directly to the surfaces of the metal electrodes, a higher conductance switching ratio can then be achieved. In contrast, when the bridging chain and the anchoring group are

separated electronically, an effective potential barrier and voltage drop will be generated between the molecular functional core and the electrode, thus reducing the switching ratio significantly.

Single-molecule devices with diarylethene

Based on the switching characteristics of photoisomerized diarylethene molecules, a one-way molecular optoelectronic switch between gold electrodes has been constructed using the MCBJ technology[26]. Because the presence of the gold electrode quenches the excited state of the diarylethene molecule in the open form, switching from a high-conductance state (closed form) to a low conductance state (open form) under visible light (546 nm) illumination was observed. However, the reverse process under ultraviolet (UV) illumination (313 nm) failed. Specifically, the energy level of the excited molecule involved in the ring-closing process is close to the Fermi level of the gold electrode, which promotes energy transfer between the molecule and the electrodes, thereby quenching the molecular excited state.

In order to overcome the quenching caused by the metal electrodes, single-molecule devices have been prepared with single-walled carbon nanotube electrodes and thiophene-based or pyrrole based diarylethenes acting as the functional molecules[27]. However, although the thiophene-based molecules can be photo-cyclized under UV irradiation, resulting in an increase in current and allowing a high level of conductance to be maintained without continuous UV irradiation, the ring-opening process is not available. In addition, the pyrrole-based device can be switched on under UV irradiation and switched back thermally under dark conditions. To enable further tailoring of the electronic structural characteristics of the single-molecule device, particularly at the molecule–electrode interface, the electrode material has been changed to graphene. A diarylethene derivative with a single methylene group (CH_2) located between the terminal amine group and the functional center on each side has been covalently bonded with graphene point contacts to form a single-molecule device[28]. Because the CH_2 group can cut off the delocalization of the π electrons, the electronic interaction between the molecule and the electrode is decoupled. Therefore, this type of device can be switched from the off state to the on state. However, the reversible configuration change between the open and closed states of the diarylethene molecule still could not be realized in this device (Fig. 1(d)). Through further introduction of three non-conjugated CH_2 groups between the diarylethene core and the anchoring amine group (Fig. 1(e)), the molecule-electrode interface coupling has been fully optimized[7]. The problem of one-way switching of diarylethene molecular electronics has also been solved. Specifically, a stable and reversible single-molecule photoelectric switch device has been constructed that has demonstrated outstanding performance in terms of accuracy (on/off ratio of 100), stability (operation for over a year), and reproducibility (46 devices with more than 100 cycles of photo-switching). Based on this realization of *in situ* reversible switching between the open and closed states, the temperature-dependent charge transport mechanism of the single-molecule switching devices and the other factors that regulate the device have been investigated. In both the open and closed forms, the device shows a transition from low-temperature coherent tunneling to high-temperature incoherent transport[14]. This occurs because of the thermally activated torsional vibration of the phenyl ring on each side of the molecule, which leads to increased vibrational coupling and also provides additional conductance channels. Because of the subtle electron–phonon coupling effect related to the energy difference between the Fermi level of the electrode and the energy level of the dominant transport molecular orbital, the incoherent transport activation energies of the device in the open and closed forms show different bias-dependent trends. In addition, the dependence of the conductivity characteristics on the molecule–electrode coupling strength has also been investigated. Through theoretical calculations, it has been found that the large conductivity difference between the open and closed states is mainly dependent on the electronic structure of the molecule itself, and has nothing to do with the electrode materials used in the devices[29].

SAM devices with diarylethene

In addition to the single-molecule devices, molecular tunneling devices formed using SAMs have also exhibited certain properties of functional molecules. For example, a molecular tunneling device based on diarylethene SAMs, a gold substrate, and a multilayer graphene top electrode has been constructed, as shown in Fig. 1(f). It is possible to observe the distinguishable differences in conductivity between the closed and open states of the diarylethene film[30]. However, in real-time measurements, only one-way switching behavior from

the open state to the closed state could be realized. By introducing reduced graphene oxide to replace the multilayer graphene as the electrode, the device successfully realized the reversible switching function, which is based on the switching state of the diarylethene molecules under alternate irradiation by UV and visible light sources[31].

In addition, a diarylethene molecular tunneling device based on nano-gapped gold electrodes has been constructed based on a monolayer of functional molecules with diarylethene photochromic units and electro-active carbon-rich ruthenium complexes on both sides. The Ru bridging group can adjust the electronic coupling between the diarylethene unit and the Au electrode to realize the reversible switching function[32]. Based on the unique orthogonally modulable characteristics of this device, light and electrochemical stimuli are used as inputs and the conductance of the molecules is regarded as the output. This combination of on/off radiation and electrolysis provides four possible outcomes and a rationally designed logic gate can thus be realized (Fig. 1(g)).

Single-molecule azobenzene switches

In addition to diarylethene, azobenzene is also used widely to construct single-molecule optoelectronic switches because of its photoinduced *cis-trans* isomerism effect, as illustrated in Fig. 2(a). For example, single molecules with azobenzene units have been covalently assembled into nano-gapped graphene point contacts to construct single-molecule optoelectronic switches. In this device type, the configurational change in the azobenzene unit occurs directly in its molecular backbone[33] (Fig. 2(c)). In another device that contained a single peptide molecule (Fig. 2(b)), an azobenzene unit with interconversion between the well-defined *cis* and disordered *trans* isomers was used as the macromolecule core unit[34]. Because of the configurational changes in azobenzene, three different conductivity states were observed that corresponded to a specific range of hydrogen bond lengths in the *cis* isomer and the specific dihedral angles in the *trans* isomer. In addition to forming the backbone of the bridging molecule, azobenzene can also be used as the side group of the bridging molecule, which undergoes configurational changes under light stimulation, as illustrated in Fig. 2(d). By connecting single molecules with an azobenzene side group to nanogapped graphene electrodes, different dipole characteristics can be observed, which are in the direction opposite to that of the terphenyl backbone with values of ~6.59 D and ~1.22 D for the *cis* and *trans* forms (Fig. 2(e)), respectively[35]. In addition, when the azobenzene unit is introduced as a side group into the central ring of the terphenyl, the polymorphism of the stereoelectronic effect of the terphenyl is further enriched[36]. As a result of the asymmetry caused by introduction of the additional configurations into the terphenyl backbone, four different conformational states appear for the azobenzene in *trans* or *cis* form, as shown in Fig. 2(f). Furthermore, the different azobenzene configurations will affect the dihedral angle between the phenyl ring close to the substituent and the central ring, and the corresponding rotation barriers. In addition to serving as the bridging molecules in single-molecule devices, azobenzene molecules can also be used in vertical tunneling SAM devices to achieve electrical conductance changes, which are caused by changes between their photoisomers. For example, a photo-switchable molecular monolayer has been constructed (Fig. 2(g)), in which one side of the monolayer is chemically covalently fixed and the other side is in physical contact between two graphene electrodes[37]. In this device, because of the photoinduced conformational change in azobenzene, the lengths of the molecular isomers change, thereby enabling realization of a stable molecular optical switch. Similar to the single-molecule devices, because the azobenzene unit that is fixed in the lateral ring undergoes photochemical *trans-cis* isomerization, azobenzene, which acts as the core of the bridging molecules (Fig. 2(h)), can also be used to modify the electronic properties of the oligothiophene chains reversibly in monolayer molecular devices[38].

Single-molecule switches with other photochromic molecules

In addition, several other photochromic molecules, including dimethyldihydropyrene, dihydroazulene, and spiropyran derivatives, can also be used as bridging molecules in single-molecule devices. Because of the photoinduced configurational changes in these materials, conductance switching can be realized. For example, when using the MCBJ technique, single-molecule junctions with dimethyldihydropyrene molecules have been fabricated successfully[39] (Fig. 3(a)). A very high ON/OFF ratio (>10^4) and excellent conductance reversibility were achieved. Among the photochromic dihydroazulene derivatives used in the single-molecule break junction,

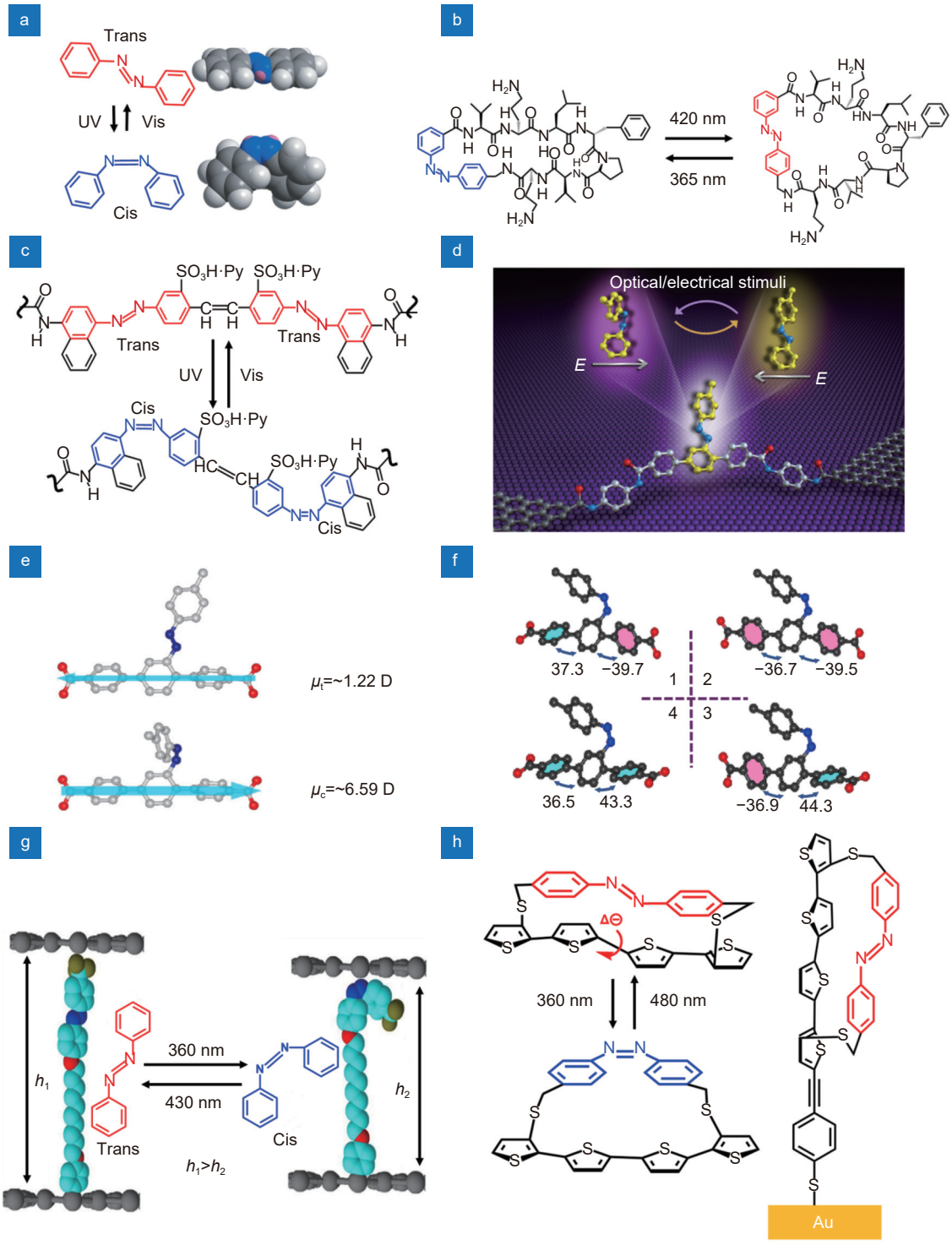

Fig. 2 | Azobenzene units used in single-molecule switches. (**a**) Structures of *trans* and *cis* isomers of azobenzene. (**b**) Azobenzene as the core unit in the macromolecule. (**c**) Chemical structures of molecules whose configurational change of the azobenzene unit occurs directly in the molecular backbone. (**d**) Schematic of azobenzene as the side group of bridging molecule in the junction. (**e**) Dipole projection on the molecular backbone. The arrow denotes the direction of the dipole projection. (**f**) Four different conformational states due to the asymmetry caused by the introduction of additional azobenzene side group in *cis* form in the terphenyl backbone. (**g**) Vertical distance between two graphene electrodes is regulated by the conformational changes in aryl azobenzene molecules with light irradiation. (**h**) Vertical tunneling self-assembled monolayer device with an azobenzene derivative on Au electrode. Figure reproduced with permission from: (a, c) ref.[33], (b) ref.[34], (f) ref.[36], John Wiley and Sons; (d, e) ref.[35], under a Creative Commons Attribution 4.0 International License; (g) ref.[37], Springer Nature; (h) ref.[38], American Chemical Society.

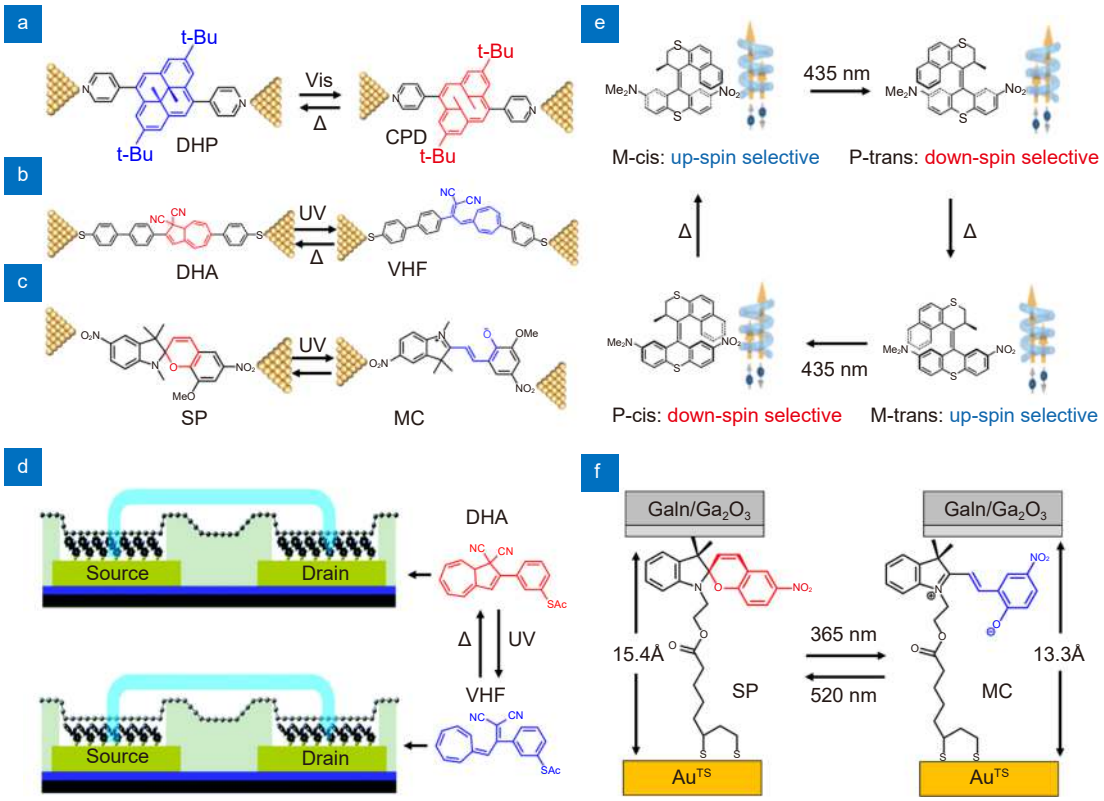

Fig. 3 | Other units used in single-molecule switches. (**a**) DHP/CPD single-molecule junction. (**b**) DHA/VHF single-molecule junction. (**c**) SP/MC single-molecule junction. (**d**) Schematic diagram of a vertical tunneling molecular switch with rGO thin films as the transparent top contact and the molecular structures of DHA and VHF. (**e**) Single-molecule switches with chirality molecules. The spin-polarization direction of the current switches with the chirality inversion. (**f**) Schematic diagram of SP SAMs in EGaIn/Ga_2O_3//SAM/Au^{TS} junctions in their open and closed forms. Figure reproduced with permission from: (a) ref.[39], American Chemical Society; (b) ref.[40], under a Creative Commons Attribution 4.0 International License; (c) ref.[41], American Chemical Society; (d) ref.[43], John Wiley and Sons; (e) refs.[19,44], under a Creative Commons Attribution 4.0 International License; (f) ref.[42], American Chemical Society.

photothermal reaction processes between the dihydroazulene and vinylheptafulvene isomers have also been observed[40] (Fig. 3(b)). Specifically, because of the introduction and shifting of the interference features during molecular conduction, both the reaction kinetics and reversibility can be detected, including the occurrence of isomerization during the reaction. Similarly, by isomerizing bifunctional spiropyran derivatives through either light or chemical stimulation, single-molecule devices can be switched quickly and reversibly between their low- and high-conductance states[41] (Fig. 3(c)). Spiropyran derivatives can be used not only in single-molecule junctions, but also in vertical molecular tunneling devices with SAMs to realize optical switching functions. Using eutectic Ga–In as the top contact layer to construct these devices, which contain a SAM of the spiropyran moiety, photoinduced switching of the conductance in the tunnel junction has been investigated[42], as shown in Fig. 3(f). As the distance of the long alkyl chain that supports the spiropyran moiety increases, the conductance switching of the spiropyran moiety is not accompanied by a significant change. Furthermore, when compared with the original spiropyran monolayer, the mixed monolayer increases the conductance switching amplitude over a range from 8 times to 35 times. This occurs because delocalization brings the positive resonances closer to the Fermi energy and broadens them, which results in higher conductivity. When a reduced graphene oxide (rGO) film was used as the interface layer between the molecule and the top metal electrode, solid-state optical switches based on monolayers composed of photo-switchable molecules have been fabricated, as shown in Fig. 3(d). In these devices, because of the structural changes in the dihydroazulene/vinylheptafulvene isomer, the conductance changes with an average ON/OFF ratio of 5–7[43]. In addition, when these molecules are replaced with chiral molecules, a solid-state spin filter device can also be realized (Fig. 3(e)), in which

the spin polarization direction can be switched using either light irradiation or thermal treatment[44]. In this device, because of the chiral-induced spin selectivity effect, the chirality inversion of the molecular motor is used as a light-driven reconfigurable spin filter.

Photoconductance of single-molecule devices

In addition to photoisomerization of the molecules, optically modulated conductance of single-molecule devices can also be achieved using excitons generated in the molecules under light irradiation, which does not involve changes in the molecular structures. Generally, because the photoinduced exciton generation process is faster than isomerization[45,46], the response times of the corresponding devices are much shorter than those of devices with isomerization, which can reach the ~ns level in theory. This is because the response time depends on the exciton dynamics. In the devices with the photo-excitons, light-excited electrons and holes are generated. As a result of Coulomb interaction, they will also form exciton binding in the molecular bridge, which results in regulation of the conductance of the single-molecule devices. For example, for single-molecule junctions that contain symmetrical perylene tetracarboxylic diimide molecules, an increase in photoconductance can be observed that is related to exciton binding formation in the molecules[47] (Fig. 4(a, c)). Specifically, when electrons are excited to move from the highest occupied molecular orbital (HOMO) to the lowest unoccupied molecular orbital (LUMO) under illumination, the holes that tunnel from the electrode toward the HOMO experience the Coulomb interaction generated by the excited electrons present in the LUMO. As a result, the HOMO level is pushed toward the Fermi level of the electrodes, thus resulting in an increase in the conductance. To improve the control of the photo-excitons on the performance of these single-molecule devices, the triplet excited states with long-lived excitation lifetimes of specific molecules have also been introduced into the devices. For example, in a three-terminal molecular transistor composed of a zinc phthalocyanine (ZnPc) functional center with alkyl chain bridging groups on both sides, the photo-excited triplet state can adjust the field-effect characteristics of the device within the incoherent limit[48]. In addition, by specifically designing molecules with a donor-acceptor structure, separation of the photogenerated electrons and holes can be promoted, thereby enhancing the ability of the photo-excitons to control the device performance. For example, single-molecule junctions with porphyrin-C_{60} donor-acceptor molecules were fabricated as shown in Fig. 4(d). Improved separation of the photo-excited charge states was found to increase the junction conductivity under light irradiation[49].

In addition to the single-molecule junctions, optical gating of molecular tunnel devices with SAMs has also been observed, thus demonstrating modulation of the photoconductivity under illumination. For example, tunneling devices containing hemicyanine dye monolayers between two Au nanowires have been constructed[50] (Fig. 4(b)). Because the conjugated portion of the SAM resonates with the Au electrode, energy transfer occurs from the plasmon of the Au electrode to the SAM, which then excites a fraction of the molecules, causing them to enter an excited state. When compared with the ground state, the delocalization of the molecular orbitals near the Fermi energy in the excited state and the cation states can effectively reduce the tunneling barrier width, thereby increasing the device conductance. To improve the photocurrent generation efficiency further, a well-designed bilayer donor-acceptor molecular junction has been proposed that offers enhanced charge separation. Unlike the tunnel junctions with a symmetrical single layer, this double-layer structure consists of covalently bonded donor and acceptor layers that allow simultaneous absorption and charge separation to occur on the covalent heterojunction. For example, in a tunnel junction composed of anthraquinone and biphenylene benzene bilayers, enhanced photoconductivity and other special properties, e.g., changes in the rectification direction and photocurrent polarity, can be observed[51] (Fig. 4(e, f)). To exclude the contribution of the plasmons induced by the metal electrode to the enhancement of the photoconductance, carbon materials are used as the electrodes to form the molecular tunnel junctions. In these junctions, the overall photoconductance enhancement originates from the molecular structures and the orbitals[52]. In addition, the effect of the molecular film thickness on the photoconductivity of the devices must also be clarified. Specifically, as the molecular layer thickness increases, the attenuation of the photocurrent intensity becomes very weak, which differs significantly

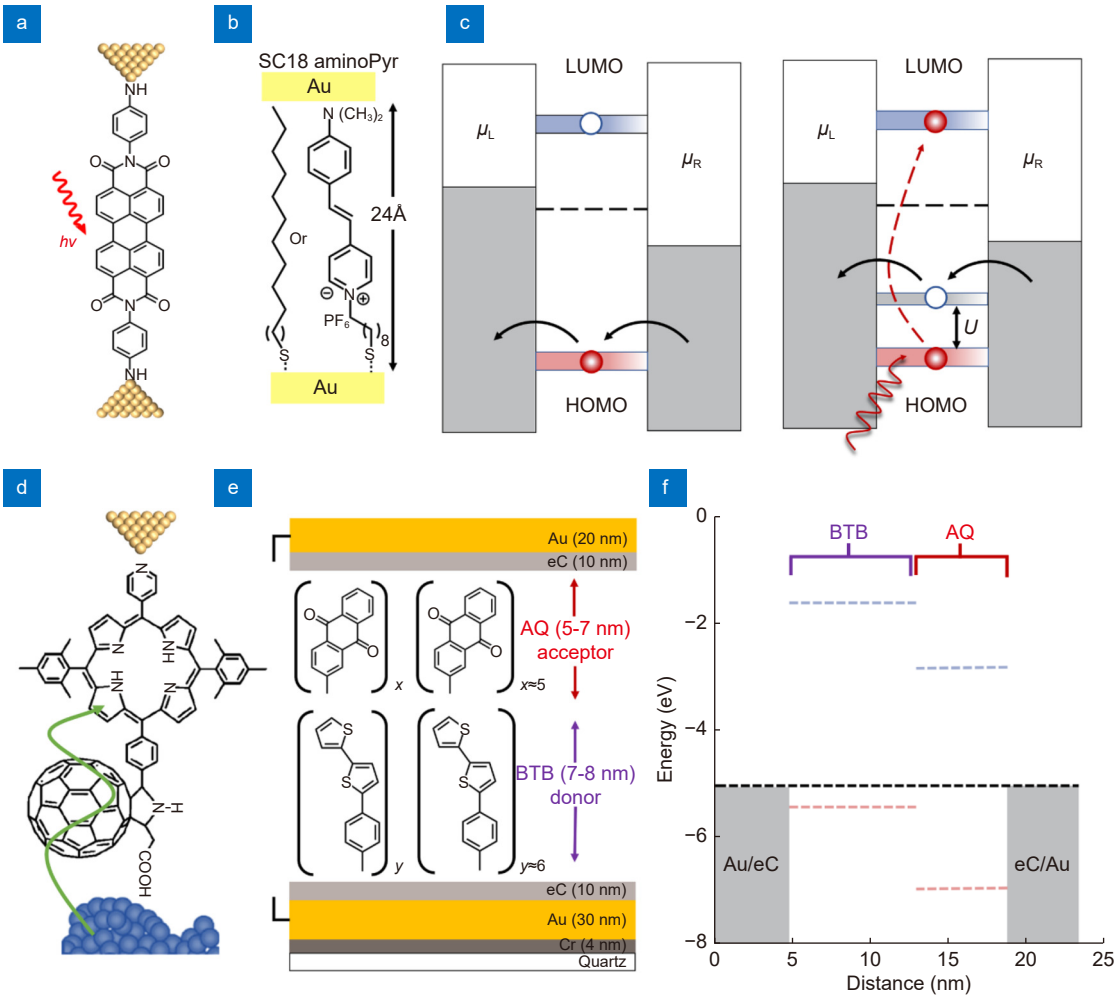

Fig. 4 | Photoconductance of single-molecule devices. (**a**) Schematic illustration of the Au/NH-PTCDI-NH/Au junction under light irradiation. (**b**) SAM-templated addressable nanogap devices comprised of AminoPyr or SC18. (**c**) Schematic presentation of the charge transport of a molecular junction affected by the excitation. (**d**) Bonding geometry of a porphyrin-C_{60} dyad molecule in the gold-ITO tunnel junction. (**e**) Schematic diagram of carbon/bilayer/carbon tunneling junctions. (**f**) Energy level diagram for a BTB–AQ bilayer junction. Figure reproduced with permission from: (a, c) ref.[47], American Chemical Society; (b) ref.[50], under a Creative Commons Attribution 4.0 International License; (d) ref.[49], American Chemical Society; (e, f) ref.[51], John Wiley and Sons.

from the exponentially decayed electronic characteristics of the same device that occur under dark conditions[53].

Plasmon-induced effects in single-molecule devices

Plasmonic effects of vacuum tunneling junctions

In single-molecule optoelectronic devices, in addition to molecular excitation, electrode excitation, in particular the generation of plasmons through interactions between the photons and free electrons on the metal electrode, can be used to regulate the charge transport in the devices. For example, because of the nonlinear tunneling conduction that occurs in the sub-nanometer gaps between the gold electrodes (Fig. 5(a)), optical rectification occurs[54]. Interestingly, a DC photocurrent will be generated when the gap is illuminated, even in the absence of any molecule. This further verifies the effect of the surface plasmons generated by metal electrodes under light illumination on the charge transport properties of these devices. In these systems, the plasmons generally regulate the charge transport properties of the devices via two mechanisms: a photo-assisted transport mechanism and a hot-electron mechanism.

Photo-assisted transport mechanism of single-molecule devices

The term photo-assisted transport mechanism means that a relative position change in the electrode energy level caused by plasmon excitation, resulting in the enhancement of the conductance or the generation of the

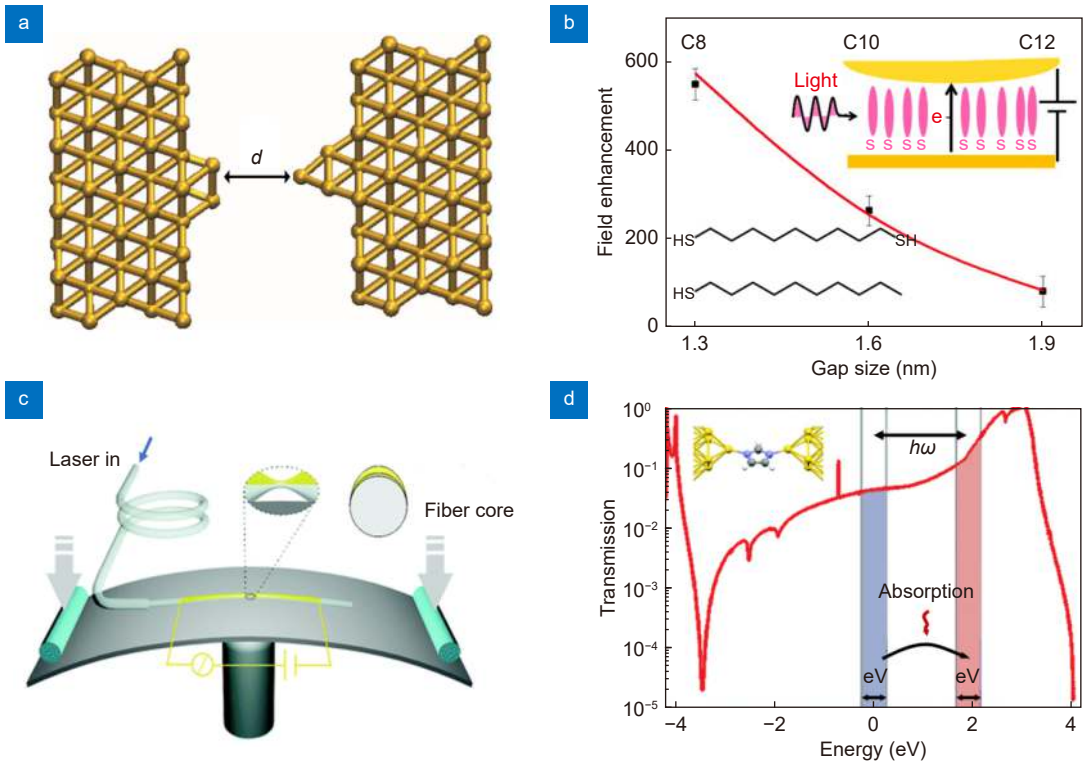

Fig. 5 | Photo-assisted transport mechanism in tunnelling junctions. (**a**) A vacuum gold tunnelling junction. (**b**) Plasmonic enhancement of the electromagnetic field in the junctions. (**c**) Schematic representation of the mechanically controllable break fiber junction chip. The inset shows a zoomed view of the suspended fiber/Cr/Au bridge. (**d**) Strong shift of the electrode energy level in imidazole single-molecule junctions caused by photon absorption. Figure reproduced with permission from: (a) ref.[54], Springer Nature; (b) ref.[55], American Chemical Society; (c, d) ref.[56], The Royal Society of Chemistry.

photocurrent, which thus leads to the change in the charge transport. It is believed that this mechanism contributes to single-molecule junction devices based on molecules for which the excitation wavelength is not in the visible light range, e.g., alkyl chain molecules. Gilad et al.[57] fabricated "suspended-wire" molecular junctions that were constructed from a SAM composed of either 1,9-nonanedithiol (C9) or decanethiol (C10) on lithographically defined Au electrodes. In the 1,9-nonanedithiol molecular junctions, photon-assisted tunneling enabled a two-time enhancement of the current to be realized (Fig. 5(b)). Similarly, using a set of junctions based on alkyl thiolated molecules with different lengths and an identical HOMO-LUMO energy gap, photocurrents were observed under laser irradiation, and the magnitude of the rectification can be used further to provide an accurate evaluation of the enhancement effect of the plasmonic field on gaps of different sizes[55]. In addition to the alkyl chain molecules, the photocurrent generation mechanism in other single-molecule devices with smaller molecules that are difficult to excite under corresponding light irradiation is also considered to be photo-assisted tunneling. For example, Xiang et al.[56] creatively developed a method in which fiber waveguides were used to irradiate a single-molecule device with light based on a mechanically controllable break junction technique to investigate the electron transport properties of single molecular junctions (Fig. 5(c) and 5(d)). They found that the strong shift in the electrode energy level caused by photon absorption led to light-induced conductance enhancement in imidazole single-molecule junctions, and proposed that the photon-assisted tunneling mechanism is strongly dependent on the transmission function characteristics of the junction. In addition, coupling of plasmon field enhancement with molecular excitation will also affect the conductance of single-molecule devices under laser irradiation at the corresponding optical frequency[58].

"Hot electron" mechanism of single-molecule devices

Although several pioneering experiments have attributed the optically induced current enhancements observed in molecular junctions to photon-assisted

tunneling, the mechanism for this conductance enhancement or photocurrent generation process remains controversial. Recently, studies have shown that hot electrons make the dominant contribution to the conductance enhancement[59]. Through a comparative analysis of photon-assisted tunneling with the hot electron mechanism, it was verified that the light-enhanced transport in 4,4′ -bipyridine single-molecule junctions was predominantly due to hot-electron transport (Fig. 6(a)). In addition, the difference between the photon-assisted tunneling and hot-electron transport mechanisms was clarified. Specifically, when the lifetime of the hot electrons is much shorter than the charge transfer time or the hot electron distribution is not generated, the optical response of the device is then caused by photon-assisted tunneling, while the hot electron emission makes the dominant contribution when the lifetime of the hot electrons is sufficiently long. Similarly, in large-area aliphatic and aromatic molecular tunnel junctions with partially transparent copper top electrodes, photocurrents have also been observed when molecular absorption has not occurred[60]. In this system, the molecules only

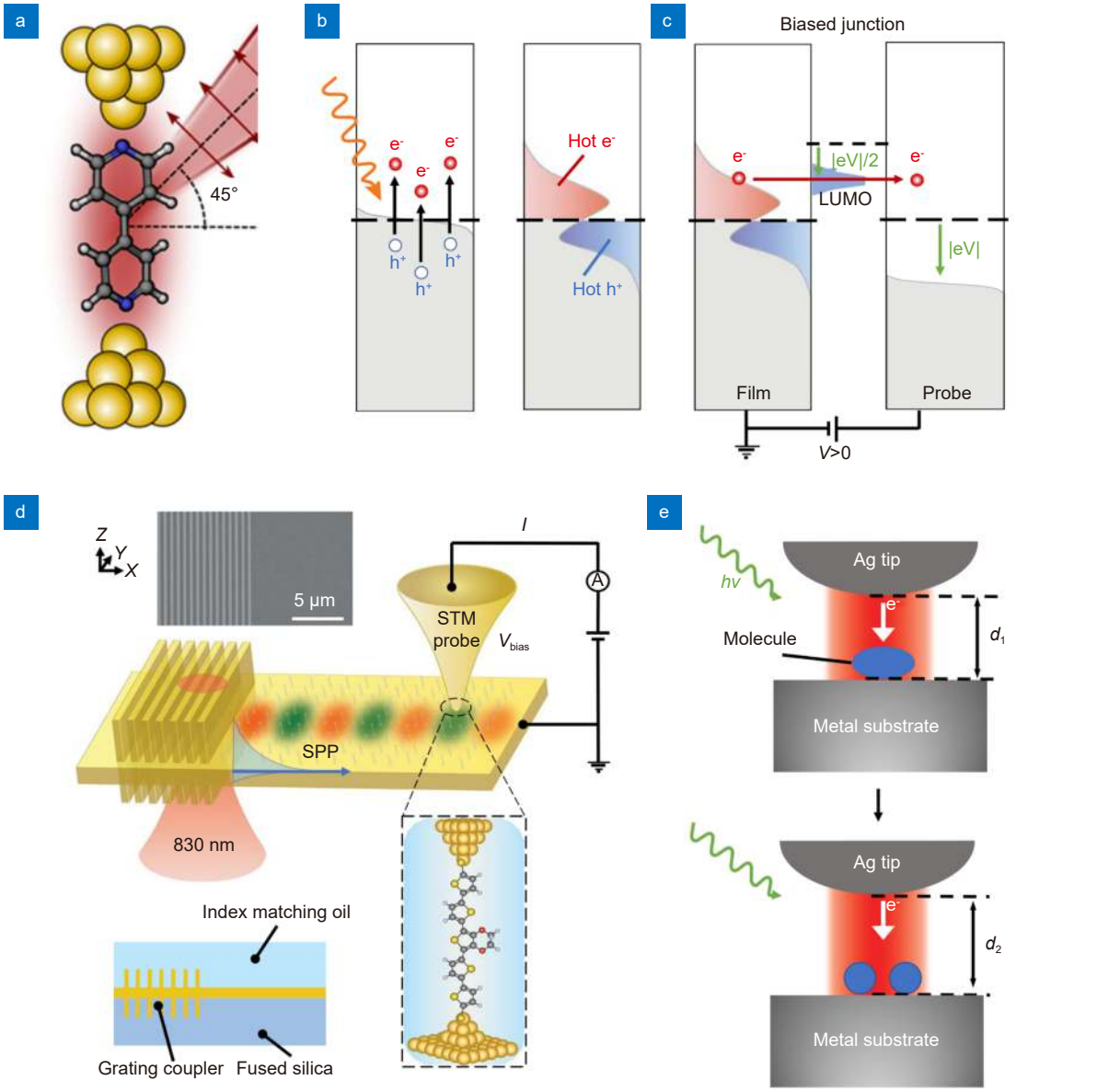

Fig. 6 | "Hot electron" effect of single-molecule devices. (**a**) Schematic demonstration of an illuminated metal-molecule-metal junction with 4,4′-bipyridine (BP) molecule. (**b**) Nonradiative decay of SPP with generated hot electrons and holes. (**c**) Nonequilibrium distribution of hot electrons and holes in biased junctions. (**d**) Experimental setup and strategy to map hot-carrier energy distributions. (**e**) Schematic illustration of the real-time observation of the plasmon-induced chemical reaction. Figure reproduced with permission from: (a) ref.[59], American Chemical Society; (b–d) ref.[62], (e) ref.[63], American Association for the Advancement of Science.

modulate the tunneling barrier, and the photocurrent is thus generated because of the hot electron excitation and emission of the copper electrode. In addition to these photoexcited hot electrons with high energy states, the thermally relaxed state after excitation also affects the charge transport through the molecules. Because of the thermal relaxation of the hot electrons (e^-) and holes (h^+) caused by Landau damping of the surface plasmon polaritons (SPPs), the thermal effect of the electrodes, particularly at the interface between the molecules and the electrodes, can then alter the conductance properties of the molecular junctions. Charge transport changes of this type in molecules within nanoscale metal gaps under illumination correspond to the temperatures of plasmonic hot spots[61]. Therefore, the plasmonic hot carrier distribution through single-molecule junctions can also be measured with spatial accuracy. For example, based on the transport mechanisms of the hot electrons and holes in the biased or unbiased junctions shown in Fig. 6(b) and 6(c), single-molecule junctions between a Au film and the Au tip of an STM setup were designed and fabricated[62], in which carefully selected molecules with different transmission characteristics were dominated by the LUMO or the HOMO. The plasmonic hot carriers were generated by the Au film with integrated grating couplers and produced different spatial distributions, as illustrated in Fig. 6(d). A major difference was observed in the current-voltage characteristics of the single-molecule junctions with and without plasmon excitation, and thus the spatial distribution of the hot carriers can be determined based on this difference.

Other effects of plasmons in single-molecule devices

In addition to the photo-assisted tunneling and hot electron mechanisms, SPPs generated from metal electrodes under illumination can also affect the charge transport of the tunneling junctions via other effects. For example, in the chemical reaction of a single dimethyl disulfide molecule, the intramolecular excitation can be enhanced by plasmons (Fig. 6(e)). This enhanced reaction process can be monitored directly using an STM in real space and real time[63]. In addition, the thermal expansion effect of the gold electrode caused by the thermal relaxation of the plasmon, rather than by the hot electron effect, can also affect the junction tunneling current by changing the morphology of the metal electrodes. This conductance adjustment caused by plasmonic heating occurs in bare metallic quantum contacts, thus indicating that atomic switches can be realized using the expansion of nanoelectrodes caused by plasmonic heating[64].

Photovoltaic effect in single-molecule devices

Although the noble metals are the most widely used contact electrode materials, nonmetallic electrodes such as semiconductor electrodes have also attracted considerable interest in single-molecule devices. Because of their specific advantages, both the molecule itself and the electrode can provide the final single-molecule junction structure with the required functions, particularly the photovoltaic function. Using the STM-BJ approach, a 1,8-nonadiene single-molecule junction with a Si-molecule-Au structure was constructed[65], and a controllable rectification function was achieved. In particular, when low-doped silicon electrodes were used, the single-molecule junction exhibited a very high rectification ratio, which then provided the basis for the photovoltaic effect[65]. Similarly, the photovoltaic properties of the GaAs-molecule-Au molecular junction have also been investigated. When a lower-doped GaAs electrode was used, the junction exhibited a higher rectification ratio, a lower dark current and higher photocurrents under application of a reverse bias voltage[66] (Fig. 7(a, b)). This is caused by the larger space charge region that occurs in the low-doped GaAs, which in turn provides a fairly high tunnel barrier to reduce the reverse bias dark current, and thus creates a larger volume to provide carriers that then contribute to the photocurrent. In response to this phenomenon, a reverse-biased junction charge transport mechanism has been proposed, in which photo-generated holes in the semiconductor tunnel into the metal through the molecular orbitals to produce the current. It should be noted here that this light response comes from the photogenerated electron-hole pairs in the semiconductor and is completely different from the molecular photoisomerization mechanism. In addition, through systematic alteration of the properties of the molecular bridges, the type and the doping density of the semiconductors, and the light intensity and wavelength, the photovoltaic behavior of the metal-molecule-GaAs junction can be finely controlled. Specifically, when compared with nonconjugated molecules, the introduction of conjugated moieties and the corresponding enhanced ohmic characteristics mean that the junctions with the saturated molecular bridges have larger rectification

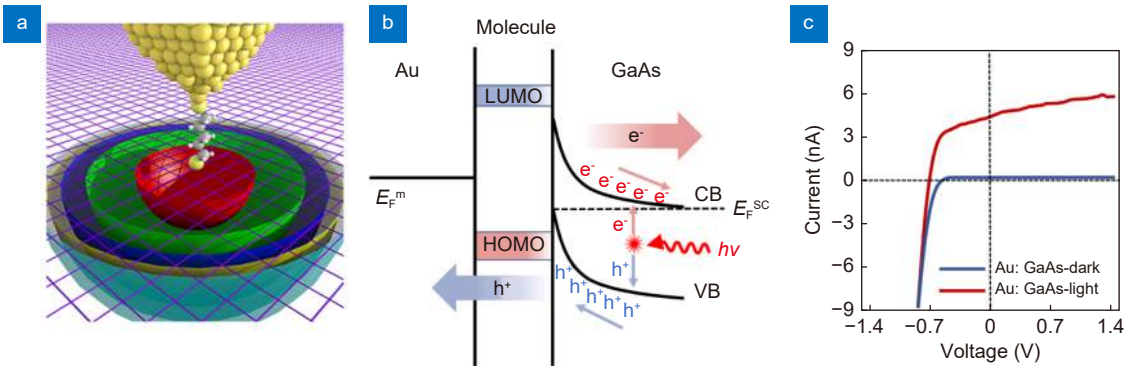

Fig. 7 | Photovoltaic effect in single-molecule devices. (**a**) A GaAs-molecule-Au molecular junction. (**b**) Schematic band diagram for the illuminated metal-molecule-semiconductor junction under reverse biases. (**c**) *I*–*V* characteristics of the Au-GaAs junction. Figure reproduced with permission from: (a, b) ref.[66], American Chemical Society; (c) ref.[67], The Royal Society of Chemistry.

characteristics and thus demonstrate better photovoltaic performance. In addition, as the voltage applied between the Au and n-GaAs electrodes increases, the rectification ratio will also increase[67] (Fig. 7(c)).

Single-molecule electroluminescence

Studies of photoelectric interactions on the molecular scale can provide a scientific basis for development of information and energy technologies in the future[68,69]. For single-molecule devices, photoelectric interaction is not only used to regulate the electrical properties of a device under illumination; the electricity can also be converted into light, which is known as single-molecule electroluminescence. Controllable realization of this single-molecule electroluminescence process serves as the experimental basis for study of the laws that govern processes such as single-molecule-level photoelectric conversion and the interactions between the molecules and fields. In addition, controllable regulation of this process is a difficult problem that researchers are determined to overcome.

Electroluminescence of plasmons

When electrons tunnel through a tunnel junction without molecules, the electroluminescence that can be observed is mainly derived from radiative decay of the surface plasmons excited by inelastic tunneling electrons[70]. Because the plasmon excitation process can be modulated by varying the topography of the metal surface, appreciable electroluminescence can be found if one of the electrode surfaces is rough. In addition, this luminescence induced by the inelastic tunneling electrons can be enhanced further by performing additional laser irradiation. This is due to the increase in the number of hot electrons caused by laser irradiation, which have energies just above the Fermi level, and the radiative decay of the hot electrons via the inelastic tunneling plasmon mode causes increased light emission[71] (Fig. 8(a)). In addition, generation of hot electrons causes the nanoscale tunnel junctions to have high reactivity and thus enables strongly confined chemical reactions, which in turn can modulate the electron tunneling processes and thereby vary the electroluminescence[72] (Fig. 8(b)). For example, Wang et al. designed and fabricated a device containing an array of electrically driven plasmonic nanorod metamaterials with a poly-l-histidine molecule tunneling layer that demonstrated hot-electron activation of oxidation/reduction reactions with O_2/H_2 molecules in its junctions[72]. The radiative decay of the surface plasmons caused by electron tunneling can also be used to monitor the reaction kinetics *in situ*. Furthermore, the plasmon intensity can be controlled via the molecular electronic properties. For example, using on-chip molecular electronic plasmon sources consisting of tunnel junctions based on SAMs sandwiched between two metal electrodes (Fig. 8(c)), localized plasmons and SPPs can be excited by the tunneling electrons (Fig. 8(d)). By varying the chemical structures of molecules with or without the molecular diode characteristics, the bias-dependent emission of the plasmons can be modulated[73] (Fig. 8(e)).

Electroluminescence of molecules in a STM nanocavity

In addition to the electrical excitation of SPPs, excitation of the molecules in a STM nanocavity can also lead to light emission. In experimental studies, the single-molecule electroluminescence process has gradually been improved. For example, in early research, C_{60} molecules

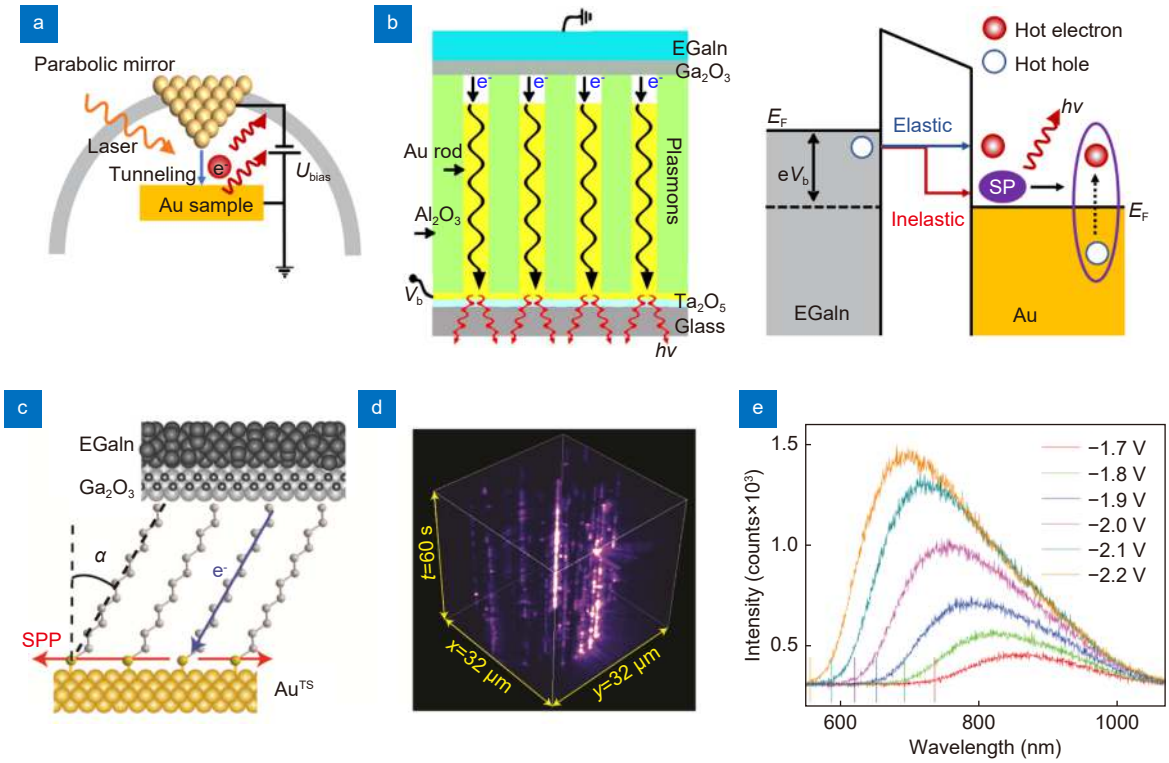

Fig. 8 | Electroluminescence of plasmon. (**a**) Photon emission induced by inelastic tunneling through a nano-gap between a sharp Au tip and an Au substrate. (**b**) Schematic diagram and mechanism diagram of how hot electrons excite plasmon electroluminescence. (**c**) Illustration of the molecular tunneling junction with a SAM of SC_n. (**d**) Blinking of plasmon sources obtained from molecular tunneling junction with a SC_{12} SAM. (**e**) Corresponding spectra of plasmon electroluminescence excited at different biases. Figure reproduced with permission from: (a) ref.[71], American Chemical Society; (b) ref.[72], (c–e) ref.[73], Springer Nature.

assembled on gold substrates were found to emit light intensely as a result of the excitation of the tunneling electrons generated by the STM tip[74]. To improve the efficiency of the electroluminescence process and undertake further investigations of the interactions between molecules and the surrounding environment, the quenching of the fluorescence by metal substrates must first be overcome. Various methods have been proposed to solve this problem. For example, in a system composed of multiple layers of molecules, because the bottom layer of molecules separates the upper layers from the substrate, the molecules on the metal substrates can be excited to emit light[75]. When individual porphyrin molecules were adsorbed on an ultrathin alumina film grown on the surface of NiAl(110) rather than via direct deposition on the metal substrate, suppressed fluorescence quenching was also achieved[76]. In addition, a method in which molecules are placed on Au(111) substrates coated with sodium chloride to overcome fluorescence quenching has also been used (Fig. 9(a) and 9(b)), and has now become a commonly used strategy[77]. In these systems, the intensity of the electroluminescence can be enhanced further using the nanocavity plasmons. Based on the same device design, by integrating the tip-enhanced Raman spectroscopy (TERS) strategy into the STM system, the structure and the chemical heterogeneity can also be correlated clearly at the single-molecule level[78].

Electroluminescence from intrinsic molecules

During single-molecule electroluminescence, direct charge transfer and energy transfer between the molecules and the substrate will cause quenching of the molecular fluorescence. To suppress this fluorescence quenching, decoupling methods have been developed that weaken the direct charge transfer and energy transfer processes between the molecules and the metal substrates. Additionally, when the plasmons are controlled to match the intrinsic energy level gap of the molecules, the electroluminescence intensity of a single molecule can be enhanced further by the nanocavity plasmon resonance that occurs in the STM tunnel junction. For example, using the decoupling effect of the sodium chloride film and the enhancement effect of the nanocavity

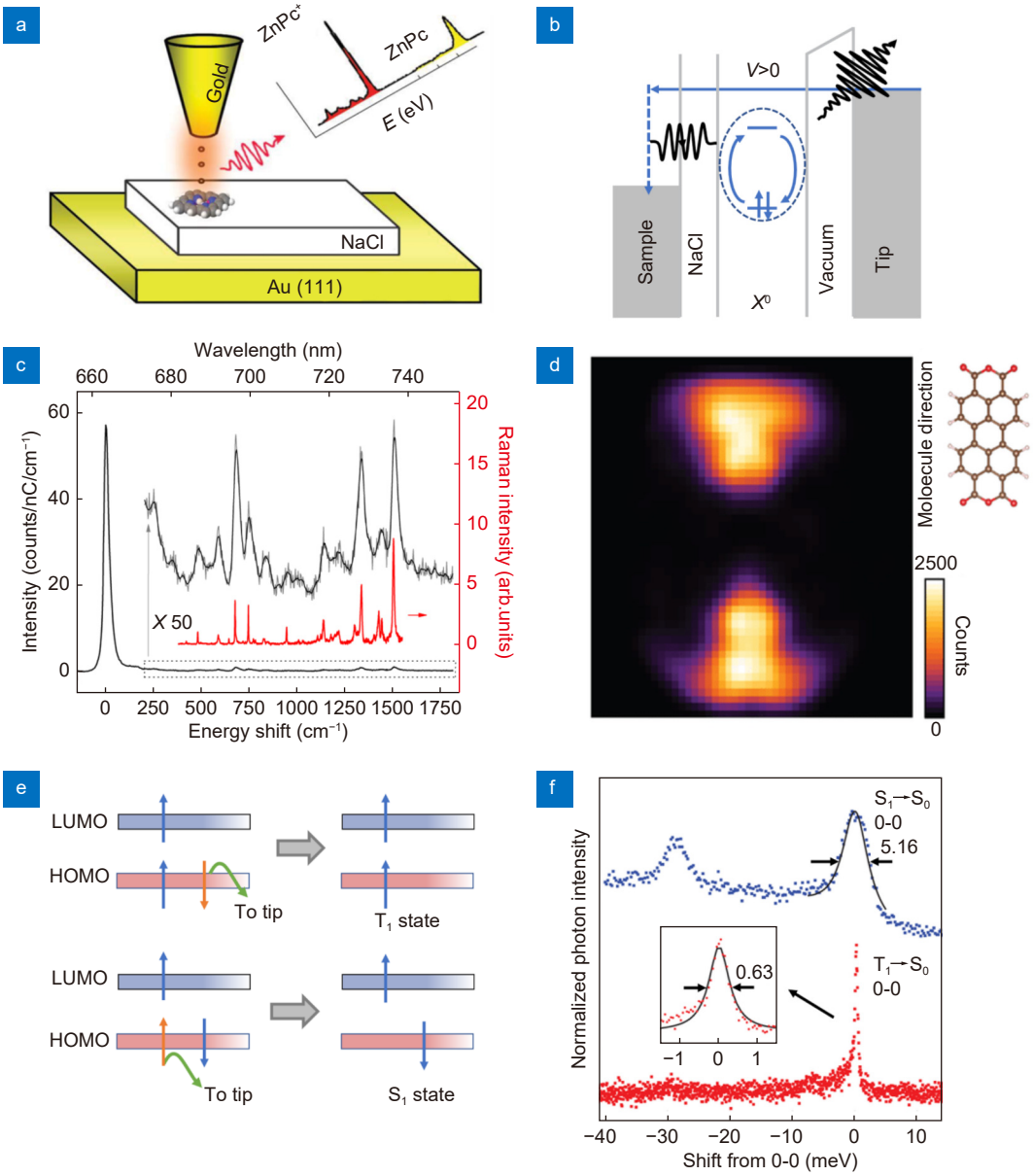

Fig. 9 | Electroluminescence from molecules in a STM nanocavity. (**a**) A single ZnPc molecule in a STM nanocavity, where the Au (111) substrate is covered with sodium chloride. (**b**) Schematic demonstration of the luminescence mechanism for a neutral ZnPc. (**c**) STM-induced light emission spectrum (black line) of the ZnPc linear tetramer. (**d**) Phosphorescence scanning tunnel luminescence map of the PTCDA/NaCl/Ag (111) system. (**e**) Schematic images of the exciton formation mechanism; the arrows represent electrons. Arrows up and down represent the direction of electron spin. (**f**) Peak characteristics of fluorescence and phosphorescence. Figure reproduced with permission from: (a, b) ref.[77], American Association for the Advancement of Science; (c) ref.[80], American Physical Society; (d−f) ref.[82], Springer Nature.

plasmon on an electrode composed of silver metal, the electroluminescence of phthalocyanine molecules deposited on NaCl/Ag (111) has been observed[79]. Using the electroluminescence spectroscopy approach, vibrational modes[80] (Fig. 9(c)), neutral and oxidized states[77], and even spin-triplet-mediated up-conversion and crossover behaviors[81] can be finely probed. When a 3,4,9,10-perylenetetracarboxylicdianhydride (PTCDA) molecule was adsorbed on a three-monolayer NaCl film on top of Ag(111), spin- triplet excitons were also observed during the electroluminescence process[82] (Fig. 9(d–f)).

Coupling of molecular electroluminescence and plasmon nanocavity

For the molecules in the nanocavity, direct excitation of nanocavity plasmons by the tunneling electrons can not only enhance the molecular electroluminescence[75], but also can induce interactions between the single

molecules and the nanocavity plasmons, which then causes the corresponding spectral characteristics of the electroluminescence to change. When the molecular illuminator interacts resonantly with the nanocavity plasmons, the coherent coupling between the discrete states of the illuminator and the continuous states of the nanocavity plasmons leads to the occurrence of Fano resonance caused by quantum interference, which results in changes in the spectral lines of the plasmons (Fig. 10(a, b)). For example, when an isolated and decoupled ZnPc molecule is located in the vicinity of a plasmon nanocavity that is being excited by tunneling electrons, the plasmons will interact with the molecule, resulting in occurrence of the Fano resonance effect[83]. This Fano resonance effect can also be achieved when the ZnPc molecule is replaced by other molecules (e.g., polycyclic aromatic hydrocarbon molecules)[84]. In addition, when the STM tip is located near the molecule, as a result of the energy transfer between the plasmon and the molecular exciton and the quantum mechanical interference effect, asymmetric dips can be observed in the broad luminescence spectrum of the plasmon[85].

Intermolecular coupling during electroluminescence

If an interaction occurs between individual molecules adsorbed on the substrate, the spectral characteristics of the corresponding single-molecule electroluminescence will differ significantly from the characteristics of the independent single molecules. For example, highly localized excitations of the molecules can be produced by electrons tunneling from the STM tip. Because of the interactions between the molecules, the resulting electroluminescence is very different at different positions, which meant that electroluminescence imaging could be used to clarify the spatial distribution of the excitonic coupling within a well-defined arrangement of several ZnPc

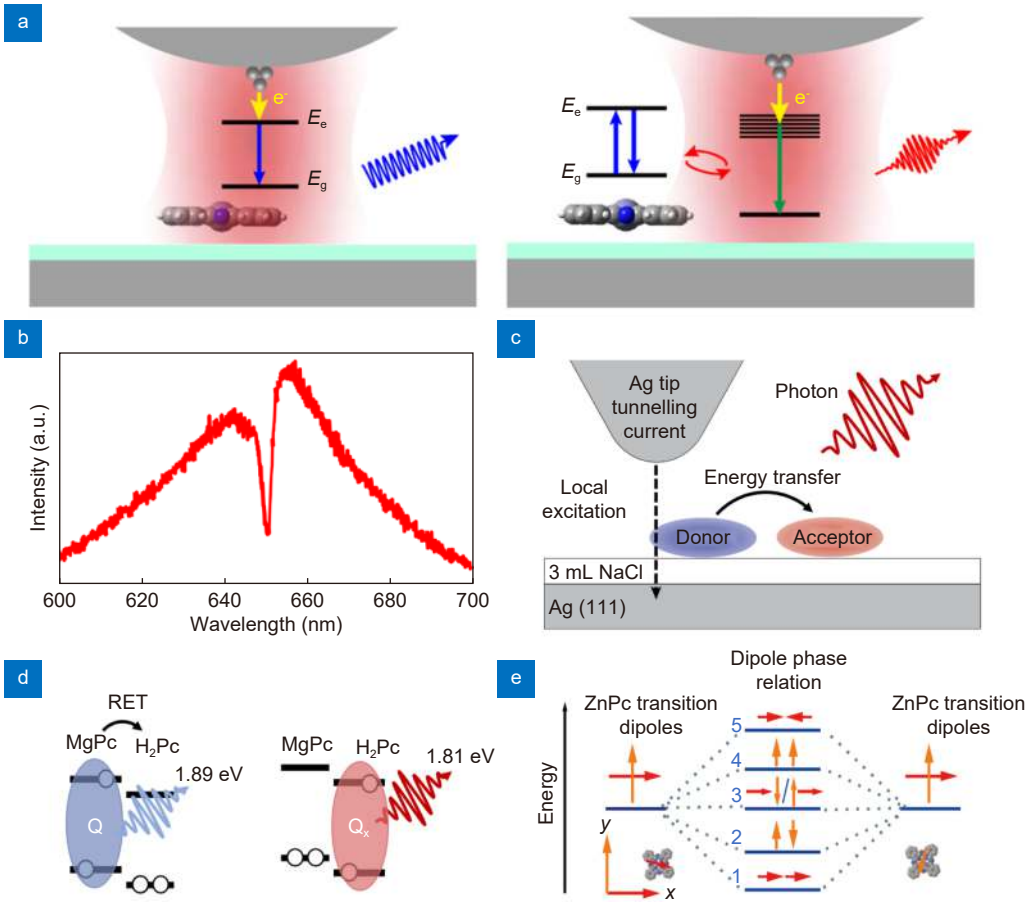

Fig. 10 | Coupling of molecular electroluminescence and plasmon nanocavity. (**a**) Two different junction structures: on top of the molecule or in close proximity to the molecule. (**b**) STM-induced luminescence of the situation that the tip is in close proximity to the molecule which cause Fano resonance. (**c**) Excitation of molecular fluorescence through intermolecular energy transfer. (**d**) Schematic illustration of the process of intermolecular energy transfer. (**e**) Exciton splitting diagram for different coherent dipole–dipole coupling modes. Figure reproduced with permission from: (a, b) ref.[83], under a Creative Commons Attribution 4.0 International License; (c, d) ref.[86], (e) ref.[87], Springer Nature.

molecules[87] (Fig. 10(e)). Furthermore, intramolecular Coulomb interactions can change the electroluminescence properties of the single molecules. Therefore, single-molecule electroluminescence based on the many-body state of the molecule can be observed[88]. In addition, as illustrated in Fig. 10(c, d), energy transfer from a magnesium phthalocyanine (MgPc) molecule to a metal-free phthalocyanine (H_2Pc) molecule has been observed in real space, which then leads to the electroluminescence of the H_2Pc molecule[86]. It should be mentioned here that, in addition to dimers, as a result of the dipole-dipole coupling of more than two molecules, interactions among multiple molecules can also lead to electroluminescence through single-exciton superradiant states. In this system, both the intermolecular interactions and the interactions between the plasmon nanocavity and the molecules exist simultaneously. The nanocavity plasmons generated by the STM tip can modify the line width and the emission intensity of the electroluminescence of the molecular chains dramatically[89].

Electroluminescence in single-molecule junctions

Although many works have reported on the single-molecule electroluminescence excited by tunneling electrons in a STM nanocavity, control of the electroluminescence of the single molecules that bridge the electrodes directly remains challenging. To realize this control, two important difficulties need to be overcome: the first problem is to determine how to cause the individual molecules to connect firmly to the electrodes and the second problem is to determine how to avoid quenching of the excited state of the molecule. For example, single-molecule junctions, in which the molecule was suspended between a metallic Au(111) surface and the STM tip, were designed as shown in Fig. 11(a). The electroluminescence of a polythiophene molecular wire could then be

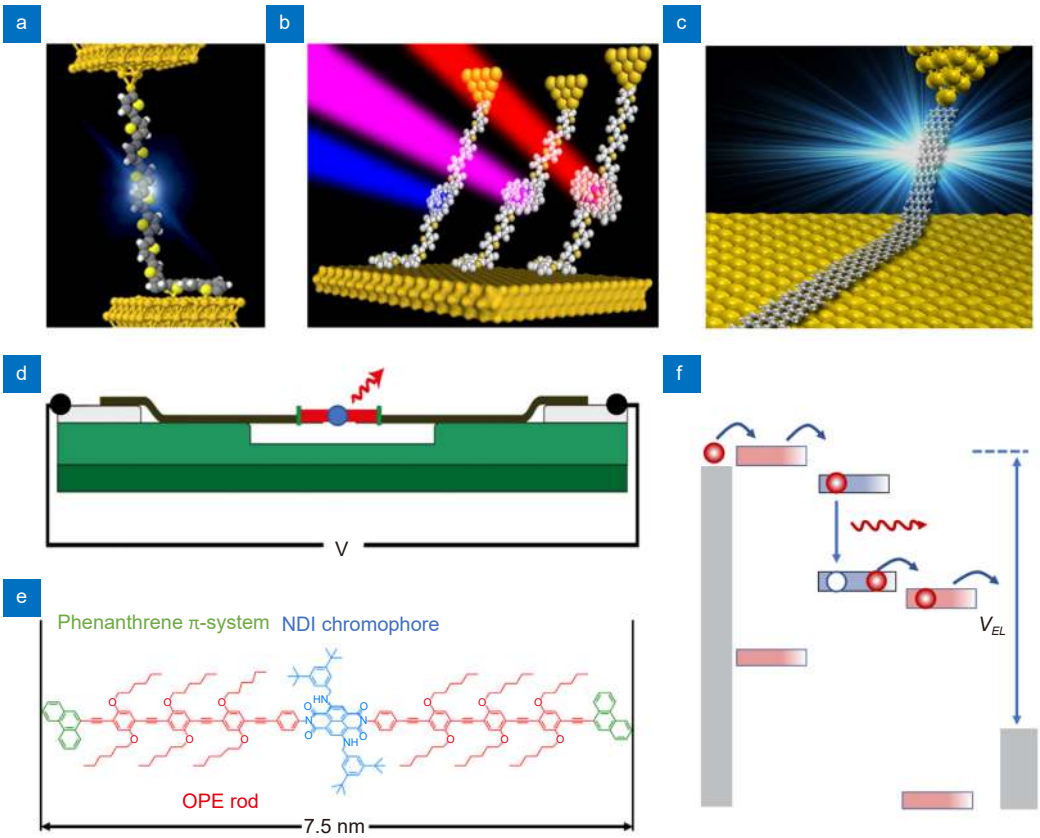

Fig. 11 | Electroluminescence in single-molecule junctions. (**a**) A polythiophene molecular wire suspended between the metal substrate and the tip of STM. (**b**) Fluorescent junctions with different emitting units suspending between the substrate and the tip of the STM by oligothiophene chains. (**c**) A single graphene nanoribbon junction. (**d**) Device structure of the nanotube–molecule–nanotube junction. (**e**) Chemical structure of the molecule, which consists of a central 2,6-dibenzylamino core-substituted NDI chromophore (blue), two OPE rods (red) and phenanthrene anchor units (green). (**f**) Energy-level model with the HOMO and LUMO molecular orbitals of the OPE and NDI subunits. Figure reproduced with permission from: (a) ref.[90], American Physical Society; (b) ref.[91], American Chemical Society; (c) ref.[92], American Chemical Society; (d–f) ref.[93], Springer Nature.

realized[90]. Furthermore, using junctions composed of different molecular emitting chromophore units suspended between a similar Au(111) surface and the STM tip by organic oligothiophene bridges (Fig. 11(b)), the color of the molecular luminescence, i.e., the molecular light emission wavelength, can be selected accurately within the 750−1000 nm range without modifying any other spectral properties[91]. When the molecule in the junction is replaced with a graphene nanoribbon (GNR) (Fig. 11(c)), the electroluminescence properties of individual GNRs can be realized, particularly with a bright narrow-band red light emission. In addition, the electroluminescence can be tuned using the bias voltage applied to the junction, which results in emission of different colors[92]. In addition to the vertical tunneling junctions fabricated in the STM, horizontal devices with carbon electrodes have also been proposed. As the electrodes, carbon materials offer advantages because of their highly tunable band gaps, atomically precise edges, and delocalized conductive electrons. For example, when a rod-like molecule is connected to two metallic single-walled carbon nanotube electrodes to form a rigid junction (Fig. 11(d, f)), an electrically triggered luminescence signal can then be obtained from the junction[93]. In addition to these single-molecule junctions, vertical molecular tunneling junctions with Au/carbon/SAM/carbon/Au structures have also been designed to produce electroluminescence. Using this system, robust bipolar bright light emission has been observed[94]. Because the wavelength of the spectrum corresponds to the energy level difference of the electronic transition, the charge transfer mechanism between the molecules can be clarified based on the emitted light spectrum.

Summary and outlook

In conclusion, the optoelectronic properties of single-molecule devices are clarified in this review. The paper not only discusses the effects of light on the electrical properties of molecular devices, but also considers the luminescence generated during molecular charge transfer. The optoelectronic mechanisms of single-molecule functional devices are summarized, with particular focus on the processes of photoisomerization, photoexcitation, and photo-assisted tunneling. In addition, the use of optoelectronic mechanisms to realize the corresponding functions of these single-molecule devices has also been proposed and implemented. For example, based on the photoisomerization of the molecules, single-molecule optoelectronic switches have been realized. Other effects, including photoconductance, plasmon-induced excitation, photovoltaic effects, and electroluminescence, have also been used to construct single-molecule functional devices.

Although significant achievements have been made in the development of single-molecule functional devices with different light-matter interactions, it will still be necessary to improve the research techniques used in the field, expand the current research systems, and explore the working mechanisms in depth to allow new applications to be realized. Specifically, infrared, terahertz or microwave band light should be introduced to explore the photoelectric interaction processes. To observe the ultra-fast photoelectron processes and chemical bond change processes of the single molecules in these devices, it will be necessary to develop a measurement technology that combines femtosecond laser techniques with electrical testing. Furthermore, polarized light can be used to control specific physical properties of single-molecule devices, e.g., spin. In addition to improving the research techniques, the existing research systems should also be expanded. For example, the photoelectron transfer processes in biological protein systems such as chlorophyll should be explored.

Based on these improved techniques and new research systems, the mechanisms of the optoelectronic effects in these single-molecule devices should be explored further. For example, the processes of photoexcitation, photoisomerization, and plasmon-induced excitation all need to be clarified further. It will be necessary to study the interaction mechanisms between the charge transport occurring in the single-molecule devices and the infrared, terahertz, and/or microwave fields. With regard to practical applications, it will be necessary to develop faster photoisomerization switches, photoconductive devices with higher efficiency, and environmentally stable single-molecule electroluminescent devices. In particular, if single-molecule electroluminescent devices can be encapsulated to satisfy sufficient stability, it is possible to be used in cells for biological applications. Furthermore, control of the light-excited quantum states in single-molecule devices must also be explored to achieve applications in fields including quantum sensing, quantum computing, and quantum communications. In addition, a breakthrough single-molecule device preparation technology with efficient molecule and electrode connection, precise nano-gap electrode preparation, and

high-density array device integration should be developed to implement integrated applications.

References

1. Xiang D, Wang XL, Jia CC, Lee T, Guo XF. Molecular-scale electronics: from concept to function. *Chem Rev* **116**, 4318–4440 (2016).
2. Sun LL, Diaz-Fernandez YA, Gschneidtner TA, Westerlund F, Lara-Avila S et al. Single-molecule electronics: from chemical design to functional devices. *Chem Soc Rev* **43**, 7378–7411 (2014).
3. Chen HL, Stoddart JF. From molecular to supramolecular electronics. *Nat Rev Mater* **6**, 804–828 (2021).
4. Hu AQ, Liu S, Zhao JY, Wen T, Zhang WD et al. Controlling plasmon-exciton interactions through photothermal reshaping. *Opto-Electron Adv* **3**, 190017 (2020).
5. Jia CC, Lin ZY, Huang Y, Duan XF. Nanowire electronics: from nanoscale to macroscale. *Chem Rev* **119**, 9074–9135 (2019).
6. Wang PQ, Jia CC, Huang Y, Duan XF. Van der Waals heterostructures by design: from 1D and 2D to 3D. *Matter* **4**, 552–581 (2021).
7. Jia CC, Migliore A, Xin N, Huang SY, Wang JY et al. Covalently bonded single-molecule junctions with stable and reversible photoswitched conductivity. *Science* **352**, 1443–1445 (2016).
8. Li PH, Jia CC, Guo XF. Structural transition dynamics in carbon electrode-based single-molecule junctions. *Chin J Chem* **39**, 223–231 (2021).
9. Bai J, Li XH, Zhu ZY, Zheng Y, Hong WJ. Single-molecule electrochemical transistors. *Adv Mater* **33**, 2005883 (2021).
10. Li PH, Jia CC, Guo XF. Molecule-based transistors: from macroscale to single molecule. *Chem Rec* **21**, 1284–1299 (2020).
11. Lee TH, Gonzalez JI, Zheng J, Dickson RM. Single-molecule optoelectronics. *Acc Chem Res* **38**, 534–541 (2004).
12. Chen LJ, Feng AN, Wang MN, Liu JY, Hong WJ et al. Towards single-molecule optoelectronic devices. *Sci China Chem* **61**, 1368–1384 (2018).
13. Garrigues AR, Wang LJ, del Barco E, Nijhuis CA. Electrostatic control over temperature-dependent tunnelling across a single-molecule junction. *Nat Commun* **7**, 11595 (2016).
14. Xin N, Jia CC, Wang JY, Wang SP, Li ML et al. Thermally activated tunneling transition in a photoswitchable single-molecule electrical junction. *J Phys Chem Lett* **8**, 2849–2854 (2017).
15. Coronado E. Molecular magnetism: from chemical design to spin control in molecules, materials and devices. *Nat Rev Mater* **5**, 87–104 (2020).
16. Jia CC, Grace IM, Wang PQ, Almeshal A, Huang ZH et al. Redox control of charge transport in vertical ferrocene molecular tunnel junctions. *Chem* **6**, 1172–1182 (2020).
17. Jia CC, Famili M, Carlotti M, Liu Y, Wang PQ et al. Quantum interference mediated vertical molecular tunneling transistors. *Sci Adv* **4**, eaat8237 (2018).
18. Famili M, Jia CC, Liu XS, Wang PQ, Grace IM et al. Self-assembled molecular-electronic films controlled by room temperature quantum interference. *Chem* **5**, 474–484 (2019).
19. Suda M, Thathong Y, Promarak V, Kojima H, Nakamura M et al. Light-driven molecular switch for reconfigurable spin filters. *Nat Commun* **10**, 2455 (2019).
20. Zhang JL, Zhong JQ, Lin JD, Hu WP, Wu K et al. Towards single molecule switches. *Chem Soc Rev* **44**, 2998–3022 (2015).
21. Li H, Qu DH. Recent advances in new-type molecular switches. *Sci Chin Chem* **58**, 916–921 (2015).
22. Yang FX, Sun LJ, Duan QX, Dong HL, Jing ZK et al. Vertical-organic-nanocrystal-arrays for crossbar memristors with tuning switching dynamics toward neuromorphic computing. *SmartMat* **2**, 99–108 (2021).
23. Liu ZH, Ren SZ, Guo XF. Switching effects in molecular electronic devices. *Top Curr Chem* **375**, 56 (2017).
24. Tam ES, Parks JJ, Shum WW, Zhong YW, Santiago-Berríos MB et al. Single-molecule conductance of pyridine-terminated dithienylethene switch molecules. *ACS Nano* **5**, 5115–5123 (2011).
25. Kim Y, Hellmuth TJ, Sysoiev D, Pauly F, Pietsch T et al. Charge transport characteristics of diarylethene photoswitching single-molecule junctions. *Nano Lett* **12**, 3736–3742 (2012).
26. Dulić D, van der Molen SJ, Kudernac T, Jonkman HT, de Jong JJD et al. One-way optoelectronic switching of photochromic molecules on gold. *Phys Rev Lett* **91**, 207402 (2003).
27. Whalley AC, Steigerwald ML, Guo XF, Nuckolls C. Reversible switching in molecular electronic devices. *J Am Chem Soc* **129**, 12590–12591 (2007).
28. Jia CC, Wang JY, Yao CJ, Cao Y, Zhong YW et al. Conductance switching and mechanisms in single-molecule junctions. *Angew Chem Int Ed* **52**, 8666–8670 (2013).
29. Han L, Zuo X, Li H, Li Y, Fang CF et al. Rational design of reversible molecular photoswitches based on diarylethene molecules. *J Phys Chem C* **123**, 2736–2745 (2019).
30. Koo J, Jang Y, Martin L, Kim D, Jeong H et al. Unidirectional real-time photoswitching of diarylethene molecular monolayer junctions with multilayer graphene electrodes. *ACS Appl Mater Interfaces* **11**, 11645–11653 (2019).
31. Kim D, Jeong H, Hwang WT, Jang Y, Sysoiev D et al. Reversible switching phenomenon in diarylethene molecular devices with reduced graphene oxide electrodes on flexible substrates. *Adv Funct Mater* **25**, 5918–5923 (2015).
32. Meng FB, Hervault YM, Shao Q, Hu BH, Norel L et al. Orthogonally modulated molecular transport junctions for resettable electronic logic gates. *Nat Commun* **5**, 3023 (2014).
33. Cao Y, Dong SH, Liu S, Liu ZF, Guo XF. Toward functional molecular devices based on graphene-molecule junctions. *Angew Chem Int Ed* **52**, 3906–3910 (2013).
34. Chen XJN, Yeoh YQ, He YB, Zhou CG, Horsley JR et al. Unravelling structural dynamics within a photoswitchable single peptide: a step towards multimodal bioinspired nanodevices. *Angew Chem Int Ed* **59**, 22554–22562 (2020).
35. Meng LN, Xin N, Hu C, Wang JY, Gui B et al. Side-group chemical gating via reversible optical and electric control in a single molecule transistor. *Nat Commun* **10**, 1450 (2019).
36. Meng LN, Xin N, Wang JY, Xu JY, Ren SZ et al. Atomically precise engineering of single-molecule stereoelectronic effect. *Angew Chem Int Ed* **60**, 12274–12278 (2021).
37. Seo S, Min M, Lee SM, Lee H. Photo-switchable molecular monolayer anchored between highly transparent and flexible graphene electrodes. *Nat Commun* **4**, 1920 (2013).
38. Lenfant S, Viero Y, Krzeminski C, Vuillaume D, Demeter D et al. New photomechanical molecular switch based on a linear π-conjugated system. *J Phys Chem C* **121**, 12416–12425 (2017).
39. Roldan D, Kaliginedi V, Cobo S, Kolivoska V, Bucher C et al. Charge transport in photoswitchable dimethyldihydropyrene-type single-molecule junctions. *J Am Chem Soc* **135**,

5974–5977 (2013).
40. Huang CC, Jevric M, Borges A, Olsen ST, Hamill JM et al. Single-molecule detection of dihydroazulene photo-thermal reaction using break junction technique. *Nat Commun* **8**, 15436 (2017).
41. Darwish N, Aragonès AC, Darwish T, Ciampi S, Díez-Pérez I. Multi-responsive photo- and chemo-electrical single-molecule switches. *Nano Lett* **14**, 7064–7070 (2014).
42. Kumar S, van Herpt JT, Gengler RYN, Feringa BL, Rudolf P et al. Mixed monolayers of spiropyrans maximize tunneling conductance switching by photoisomerization at the molecule-electrode interface in EGaIn junctions. *J Am Chem Soc* **138**, 12519–12526 (2016).
43. Li T, Jevric M, Hauptmann JR, Hviid R, Wei ZM et al. Ultrathin reduced graphene oxide films as transparent top-contacts for light switchable solid-state molecular junctions. *Adv Mater* **25**, 4164–4170 (2013).
44. Naaman R, Waldeck DH. Chiral-induced spin selectivity effect. *J Phys Chem Lett* **3**, 2178–2187 (2012).
45. Yao YF, Chen YS, Wang HL, Samorì P. Organic photodetectors based on supramolecular nanostructures. *SmartMat* **1**, e1009 (2020).
46. Wang YS, Yang J, Gong YX, Fang MM, Li Z et al. Host–guest materials with room temperature phosphorescence: tunable emission color and thermal printing patterns. *SmartMat* **1**, e1006 (2020).
47. Zhou JF, Wang K, Xu BQ, Dubi Y. Photoconductance from exciton binding in molecular junctions. *J Am Chem Soc* **140**, 70–73 (2018).
48. Fu B, Mosquera MA, Schatz GC, Ratner MA, Hsu LY. Photoinduced anomalous coulomb blockade and the role of triplet states in electron transport through an irradiated molecular transistor. *Nano Lett* **18**, 5015–5023 (2018).
49. Battacharyya S, Kibel A, Kodis G, Liddell PA, Gervaldo M et al. Optical modulation of molecular conductance. *Nano Lett* **11**, 2709–2714 (2011).
50. Pourhossein P, Vijayaraghavan RK, Meskers SCJ, Chiechi RC. Optical modulation of nano-gap tunnelling junctions comprising self-assembled monolayers of hemicyanine dyes. *Nat Commun* **7**, 11749 (2016).
51. Smith SR, McCreery RL. Photocurrent, photovoltage, and rectification in large-area bilayer molecular electronic junctions. *Adv Electron Mater* **4**, 1800093 (2018).
52. Najarian AM, Bayat A, McCreery RL. Orbital control of photocurrents in large area all-carbon molecular junctions. *J Am Chem Soc* **140**, 1900–1909 (2018).
53. Najarian AM, McCreery RL. Long-range activationless photostimulated charge transport in symmetric molecular junctions. *ACS Nano* **13**, 867–877 (2019).
54. Ward DR, Hüser F, Pauly F, Cuevas JC, Natelson D. Optical rectification and field enhancement in a plasmonic nanogap. *Nat Nanotechnol* **5**, 732–736 (2010).
55. Arielly R, Ofarim A, Noy G, Selzer Y. Accurate determination of plasmonic fields in molecular junctions by current rectification at optical frequencies. *Nano Lett* **11**, 2968–2972 (2011).
56. Zhao ZK, Guo CY, Ni LF, Zhao XY, Zhang SR et al. *In situ* photoconductivity measurements of imidazole in optical fiber break-junctions. *Nanoscale Horiz* **6**, 386–392 (2021).
57. Noy G, Ophir A, Selzer Y. Response of molecular junctions to surface plasmon polaritons. *Angew Chem Int Ed* **49**, 5734–5736 (2010).
58. Vadai M, Nachman N, Ben-Zion M, Bürkle M, Pauly F et al. Plasmon-induced conductance enhancement in single-molecule junctions. *J Phys Chem Lett* **4**, 2811–2816 (2013).
59. Fung ED, Adak O, Lovat G, Scarabelli D, Venkataraman L. Too hot for photon-assisted transport: hot-electrons dominate conductance enhancement in illuminated single-molecule junctions. *Nano Lett* **17**, 1255–1261 (2017).
60. Fereiro JA, McCreery RL, Bergren AJ. Direct optical determination of interfacial transport barriers in molecular tunnel junctions. *J Am Chem Soc* **135**, 9584–9587 (2013).
61. Nachman N, Selzer Y. Thermometry of plasmonic heating by inelastic electron tunneling spectroscopy (IETS). *Nano Lett* **17**, 5855–5861 (2017).
62. Reddy H, Wang K, Kudyshev Z, Zhu LX, Yan S et al. Determining plasmonic hot-carrier energy distributions via single-molecule transport measurements. *Science* **369**, 423–426 (2020).
63. Kazuma E, Jung J, Ueba H, Trenary M, Kim Y. Real-space and real-time observation of a plasmon-induced chemical reaction of a single molecule. *Science* **360**, 521–526 (2018).
64. Zhang WQ, Liu HS, Lu JS, Ni LF, Liu HT et al. Atomic switches of metallic point contacts by plasmonic heating. *Light Sci Appl* **8**, 34 (2019).
65. Aragonès AC, Darwish N, Ciampi S, Sanz F, Gooding JJ et al. Single-molecule electrical contacts on silicon electrodes under ambient conditions. *Nat Commun* **8**, 15056 (2017).
66. Vezzoli A, Brooke RJ, Higgins SJ, Schwarzacher W, Nichols RJ. Single-molecule photocurrent at a metal-molecule-semiconductor junction. *Nano Lett* **17**, 6702–6707 (2017).
67. Vezzoli A, Brooke RJ, Ferri N, Brooke C, Higgins SJ et al. Charge transport at a molecular GaAs nanoscale junction. *Faraday Discuss* **210**, 397–408 (2018).
68. Kuhnke K, Große C, Merino P, Kern K. Atomic-scale imaging and spectroscopy of electroluminescence at molecular interfaces. *Chem Rev* **117**, 5174–5222 (2017).
69. Rosławska A, Leon CC, Grewal A, Merino P, Kuhnke K et al. Atomic-scale dynamics probed by photon correlations. *ACS Nano* **14**, 6366–6375 (2020).
70. Persson BNJ, Baratoff A. Theory of photon emission in electron tunneling to metallic particles. *Phys Rev Lett* **68**, 3224–3227 (1992).
71. Wang X, Braun K, Zhang D, Peisert H, Adler H et al. Enhancement of radiative plasmon decay by hot electron tunneling. *ACS Nano* **9**, 8176–8183 (2015).
72. Wang P, Krasavin AV, Nasir ME, Dickson W, Zayats AV. Reactive tunnel junctions in electrically driven plasmonic nanorod metamaterials. *Nat Nanotechnol* **13**, 159–164 (2018).
73. Du W, Wang T, Chu HS, Wu L, Liu RR et al. On-chip molecular electronic plasmon sources based on self-assembled monolayer tunnel junctions. *Nat Photonics* **10**, 274–280 (2016).
74. Berndt R, Gaisch R, Gimzewski JK, Reihl B, Schlittler RR et al. Photon emission at molecular resolution induced by a scanning tunneling microscope. *Science* **262**, 1425–1427 (1993).
75. Dong ZC, Zhang XL, Gao HY, Luo Y, Zhang C et al. Generation of molecular hot electroluminescence by resonant nanocavity plasmons. *Nat Photonics* **4**, 50–54 (2010).
76. Qiu XH, Nazin GV, Ho W. Vibrationally resolved fluorescence excited with submolecular precision. *Science* **299**, 542–546 (2003).
77. Doppagne B, Chong MC, Bulou H, Boeglin A, Scheurer F et al.

Electrofluorochromism at the single-molecule level. *Science* **361**, 251–255 (2018).
78. Xu JY, Zhu X, Tan SJ, Zhang Y, Li B et al. Determining structural and chemical heterogeneities of surface species at the single-bond limit. *Science* **371**, 818–822 (2021).
79. Zhang L, Yu YJ, Chen LG, Luo Y, Yang B et al. Electrically driven single-photon emission from an isolated single molecule. *Nat Commun* **8**, 580 (2017).
80. Doppagne B, Chong MC, Lorchat E, Berciaud S, Romeo M et al. Vibronic spectroscopy with submolecular resolution from STM-induced electroluminescence. *Phys Rev Lett* **118**, 127401 (2017).
81. Chen G, Luo Y, Gao HY, Jiang J, Yu YJ et al. Spin-triplet-mediated up-conversion and crossover behavior in single-molecule electroluminescence. *Phys Rev Lett* **122**, 177401 (2019).
82. Kimura K, Miwa K, Imada H, Imai-Imada M, Kawahara S et al. Selective triplet exciton formation in a single molecule. *Nature* **570**, 210–213 (2019).
83. Zhang Y, Meng QS, Zhang L, Luo Y, Yu YJ et al. Sub-nanometre control of the coherent interaction between a single molecule and a plasmonic nanocavity. *Nat Commun* **8**, 15225 (2017).
84. Kröger J, Doppagne B, Scheurer F, Schull G. Fano description of single-hydrocarbon fluorescence excited by a scanning tunneling microscope. *Nano Lett* **18**, 3407–3413 (2018).
85. Imada H, Miwa K, Imai-Imada M, Kawahara S, Kimura K et al. Single-molecule investigation of energy dynamics in a coupled plasmon-exciton system. *Phys Rev Lett* **119**, 013901 (2017).
86. Imada H, Miwa K, Imai-Imada M, Kawahara S, Kimura K et al. Real-space investigation of energy transfer in heterogeneous molecular dimers. *Nature* **538**, 364–367 (2016).
87. Zhang Y, Luo Y, Zhang Y, Yu YJ, Kuang YM et al. Visualizing coherent intermolecular dipole-dipole coupling in real space. *Nature* **531**, 623–627 (2016).
88. Miwa K, Imada H, Imai-Imada M, Kimura K, Galperin M et al. Many-body state description of single-molecule electroluminescence driven by a scanning tunneling microscope. *Nano Lett* **19**, 2803–2811 (2019).
89. Luo Y, Chen G, Zhang Y, Zhang L, Yu YJ et al. Electrically driven single-photon superradiance from molecular chains in a plasmonic nanocavity. *Phys Rev Lett* **122**, 233901 (2019).
90. Reecht G, Scheurer F, Speisser V, Dappe YJ, Mathevet F et al. Electroluminescence of a polythiophene molecular wire suspended between a metallic surface and the tip of a scanning tunneling microscope. *Phys Rev Lett* **112**, 047403 (2014).
91. Chong MC, Sosa-Vargas L, Bulou H, Boeglin A, Scheurer F et al. Ordinary and hot electroluminescence from single-molecule devices: controlling the emission color by chemical engineering. *Nano Lett* **16**, 6480–6484 (2016).
92. Chong MC, Afshar-Imani N, Scheurer F, Cardoso C, Ferretti A et al. Bright electroluminescence from single graphene nanoribbon junctions. *Nano Lett* **18**, 175–181 (2018).
93. Marquardt CW, Grunder S, Błaszczyk A, Dehm S, Hennrich F et al. Electroluminescence from a single nanotube-molecule-nanotube junction. *Nat Nanotechnol* **5**, 863–867 (2010).
94. Tefashe UM, Nguyen QV, Lafolet F, Lacroix JC, McCreery RL. Robust bipolar light emission and charge transport in symmetric molecular junctions. *J Am Chem Soc* **139**, 7436–7439 (2017).

Acknowledgements

We acknowledge primary financial supports from the National Key R&D Program of China (2017YFA0204901, 2021YFA1200101 and 2021YFA1200102), the National Natural Science Foundation of China (22150013, 21727806, 21933001 and 22173050), the Tencent Foundation through the XPLORER PRIZE and "Frontiers Science Center for New Organic Matter" at Nankai University (63181206).

Author contributions

All authors commented on the manuscript. P. H. Li, Y. J. Chen, B. Y. Wang and M. M. Li prepared the first draft of the manuscript. X. F. Guo, C. C. Jia and D. Xiang supervised the work.

Competing interests

The authors declare no competing financial interests.